1

Upcycling Plastic Waste into Graphite Using Graphenic Additives: Yield, Quality and Interaction Mechanisms via Experimentation and Molecular Dynamics

Akshay Gharpure*¹, Malgorzata Kowalik², Randy Vander Wal¹ and Adri van Duin²

¹ John and Willie Leone Family Department of Energy and Mineral Engineering and the EMS Energy Institute, Pennsylvania State University, University Park, PA 16802, USA.

² The Department of Mechanical Engineering, Pennsylvania State University, University Park, PA 16802, USA.

* Correspondence: apg86@psu.edu

Abstract

This research presents pioneering work on transforming a variety of waste plastic into synthetic graphite of high quality and purity. Six recycled plastics in various forms were obtained – including reprocessed polypropylene, high-density polyethylene flakes, shredded polyethylene films, reprocessed polyethylene (all obtained from Pennsylvania Recycling Markets Center), polystyrene foams and polyethylene terephthalate bottles (both sourced from a local recycling bin). The waste plastics were carbonized in sealed tubing reactors. The study shows that this versatile process can be used on a mix of waste plastics in a variety of recycled forms to obtain a uniform graphitic carbon phase, hence addressing the challenges of separation and transportation faced by the plastic recycling industry. The conversion yield to elemental carbon for recycled plastics was improved by up to 250% by using graphene oxide (GO) additives. Five different grades of GO and graphene were used to gain insights into the interaction mechanisms between plastics and GO during pyrolysis. The effect of GO additives on carbonization was analyzed using thermogravimetric analysis / differential scanning calorimetry and ReaxFF-based reactive molecular dynamics simulations. The obtained cokes were graphitized at 2500 °C and the graphitic quality of the synthetic graphites was analyzed using X-ray diffraction, transmission electron microscopy, and Raman spectroscopy. The plastic waste-derived synthetic graphites exhibit remarkable graphitic quality with crystallite sizes comparable with a model graphitizable material – anthracene coke. The thin, flake-like morphology and nanostructure featuring well-stacked contiguous lamellae make these graphitic carbons highly promising candidates for energy storage applications. Based

on our experiments and atomistic-scale simulations we propose interaction mechanisms between the plastic polymers and the graphenic additives that explain the chemical conversion pathways for GO-assisted waste plastic carbonization and graphitization.

Introduction

In the United States, approximately 37 million tons of plastic are used every year ^{1,2}. Of this, packing and food-service plastics represent about 16 million tons, and these are typically "single use." On average, Americans consume 100 pounds per person, per year, of packaging and food-service plastics. Globally, 300 million tons of plastic are produced every year, half of which are single-use ³. The main resin types found in these packaging and food-service applications are PET (polyethylene terephthalate, used in soft-drink bottles), HDPE (high-density polyethylene, used in milk jugs), LDPE (low-density polyethylene, used in plastic bags, containers, films, and wraps), and PP (polypropylene, used in yogurt containers and bottle caps). Together, these polymers make up approximately 85 percent of the single-use volume. Only approximately 12 percent of this material is recycled. Another 16 percent is combusted with municipal trash, from which the heat value is recovered, but the majority—more than 70 percent, or 11 million tons—is sent to landfills ⁴. Adding to the severity, more than 8 million tons of plastic waste ends up in ocean ⁵ contributing to the death of a million birds and 100,000 mammals annually ⁶. Additionally, most synthetic plastics are made from petrochemicals which have associated environmental impact and extraction and refining costs. Thus exists a huge opportunity to upcycle plastic waste into high-value carbon materials.

Concurrent with the challenge of ever-growing plastic waste, there are substantial challenges associated with graphite supply shortfall and declining availability of high-quality graphitic carbon precursors. Clean energy technology will drive demand for carbon in direct drive motors and as energy storage media ⁴. Present electric vehicles (EVs) require up to 70 kgs of graphite, even more for some models like the Tesla Model S. Every million EVs, which is about 1% of the new car market, require on the order of 75,000 tons of natural graphite to make the lithium-ion batteries (LIBs) which represents a potential ten percent increase in flake graphite demand. Because of the small size of the flake graphite market, even modest, conservative EV adoption rates will have a big effect on demand and price. Lithium-ion battery manufacturing capacity currently under

construction would require flake graphite production to more than double by 2025 ⁷. The end cost is not so much driven by the material but rather by the purification process. Recycling old LiB to retrieve graphite will not solve this because of the extensive purification process required for degraded graphite in end-of-life batteries ⁸.

Integrating renewable energy access will require grid-level storage. Graphite is the anode material for present Li-ion battery technology and also for other potential battery chemistries utilizing silicon ⁹ or based on sulfur ¹⁰. The envisioned battery-based systems will far outweigh available mined natural graphite and manufactured synthetic graphite. Notably, the price of high-carbon-purity synthetic graphite presently ranges from US\$7000 per ton to US\$20,000 per metric ton, depending on its exact properties ⁸. Moreover, related graphene applications are vast ¹¹. Other applications range from films to composites depending on graphene scale, price, and quality. Several processes are well-proven to produce graphene from graphite ¹². Therein graphite derived from plastic waste may be a high-quality source for graphene given its higher purity and uniformity compared to natural graphite.

There exist several challenges with traditional plastic recycling methods. Mechanical recycling requires a high-purity waste stream because the incompatibility of different resins and additives makes processing difficult and inefficient. The required sorting makes processing difficult and inefficient. Furthermore, the properties of mechanically recycled and reheated plastics degrade each time because of chain scission, crosslinking, thermo-oxidation, or chemical breakdown. Grinding or remelting crosslinked plastics is challenging while recycling plastics can be hampered by the presence of additives. Several chemical recycling alternatives such as depolymerization, feedstock recycling, and purification have been studied ¹³. The depolymerization approach involves breaking down plastics to obtain monomers, but it is only suitable for condensation polymers such as polyester and nylon. A strong backbone and susceptibility to chain scission make monomer recovery by depolymerization from polymers like PE and PP less suitable. The traditional feedstock recycling approaches including pyrolysis, hydrothermal treatment, and gasification are energy-intensive and downcycling processes generating lower-value products like waxes, liquid fuels or feedstock gases that compete with cannot compete with crude oil products. Enhancing the efficiency and product selectivity of feedstock recycling often necessitates the substantial utilization of catalysts, presenting its unique set of challenges, including issues related

to deactivation, disposal, and economic feasibility. Perhaps the biggest hindrance in all traditional downcycling approaches is that its economics cannot compete with virgin material. Few upcycling approaches exist today, such as turning PET into polyester textiles. Upcycling abundant plastic waste to supply the growing graphite demand will contribute to the circular economy, preserving resources, saving energy, and reducing the life cycle of CO₂.

Obtaining solid carbon from thermoplastics requires stabilization because these plastics typically crack into light gases through chain unzipping and β -bond scission. Pyrolysis of plastics in an open system under inert generates a large number of paraffinic and olefinic light gases with negligible carbon residue ^{14,15}. The general mechanism includes chain breaking, C-H bond cleavage, free radical recombination, and dismutation ¹⁶. Thermal decomposition of polyolefins typically starts around 300 °C with random scission of the polymer chain into two primary radicals. These radicals can undergo β -scission to produce light gas or intramolecular hydrogen transfer can convert these radicals into more stable secondary radicals. These secondary radicals either further continue unzipping through β -scission to form smaller olefins or form paraffins through intermolecular hydrogen transfer ^{14,17}. Plastics containing an aromatic ring in the chain undergo a similar decomposition pathway but produce fragments retaining aromatic rings. For example, the main pyrolysis products of polystyrene include styrene dimer, styrene trimer, and small molecular species such as toluene, allyl benzene, diphenylmethane, etc.

As prior studies show, oxidative stabilization is necessary to prevent this volatilization ¹⁸. Prior studies have attempted to obtain solid carbon materials from plastics by utilizing catalysts in the form of metals ¹⁹, acids ²⁰, or reactive heteroatoms ^{21,22}. However, such stabilization comes with the attendant problem of introducing impurities – requiring difficult and intensive extraction, particularly when the carbon is intended for electrochemical applications. This is in fact a limitation on the use of natural (mined) graphite for LiB use ²³. An alternative approach, well known in carbon fiber manufacture is oxidative stabilization wherein mild oxidation incorporates oxygen into the polymer matrix whereupon during carbonization radicals form resulting in polymer chains crosslinking ¹⁸. While oxidation-assisted carbonization boosts conversion yield to elemental carbon (carbon yield), it limits the graphitizing potential due to restrictive crosslinking.

To gain a better understanding of the molecular transformation characteristic of the carbonization process various modeling approaches can be utilized. Saha et al. ²⁴ used ReaxFF-based reactive atomistic molecular dynamics to evaluate the possible mechanisms for the elimination of the gaseous molecules during the carbonization process for polyacrylonitrile (PAN) and later also considered a possible templating effect of the additives, such as carbon nanotube or graphite nanoparticle ²⁵. Dasai et al. ²⁶ proposed a model for predicting the cross-sectional microstructure characteristic of the PAN-based carbon fiber based on a combined kinetic Monte Carlo and molecular dynamics approach. The ReaxFF reactive atomistic approach was also applied by other authors to get a better understanding of the carbonization process for multiple other polymers, such as poly(p-phenylene-2,6-benzobisoxazole) ²⁷, oxidized PAN ^{28,29}, or polyamide ³⁰.

In this study, we investigate an innovative approach of utilizing GO as a templating agent to increase the yield and graphitic quality of carbon obtained from waste plastics. Presently there is very little known about the mechanisms of interaction between GO and decomposing waste plastics and their effect on the graphitic quality of the obtained solid carbon. To the best of our knowledge, this is the first comprehensive work to investigate upcycling a variety of waste plastics into high-quality synthetic graphite without using heterogeneous catalysts. Upcycling overabundant plastic waste into graphitic carbons would support the renewable energy transition while reducing pollution, cost, and CO₂ emissions.

Methods

2.1 Materials

Four recycled plastics – reprocessed polypropylene (PP), high-density polyethylene (HDPE) flakes, shredded mixed polyethylene (PE) films, and mixed PE post-consumer recycled (PCR) reprocessed pellets were obtained from Pennsylvania Recycling Markets Center. Additionally, polystyrene foams and polyethylene terephthalate bottles were collected from local recycling bins. Images of the recycled plastic forms are given in the supplementary information. A blend of 50% recycled PE and 50% recycled PS was also prepared to test the behavior of mixed plastics. GO was selected as an additive with its oxygen functional groups providing the necessary stabilization while the sp² framework provides a template for the ordered growth of the surrounding carbon. Five different types of GOs with varying lateral size, stacking, and oxygen content have been used

in this study to identify mechanisms of interaction between GO and plastics. Based on the characteristics, several pairs of GO additives were identified to isolate the effect of a single parameter while keeping the other parameters constant. The following commercially available GOs were added to PE to study the effect of GO parameters on yield and graphitic quality.

- 1. Cheaptubes' few layers GO (GO1) 0.3 to 0.8 μm size, 32 wt% oxygen, and 2 to 4 stacking layers.
- 2. Cheaptubes' single layer GO (GO2) 0.3 to 0.8 μm size, 32 wt% oxygen, and 1 to 2 stacking layers.
- 3. Cheaptubes' reduced single layer GO (GO3) 0.3 to 0.8 μm size, 15 wt% oxygen, and 1 to 2 stacking layers.
- 4. Graphene Supermarket's high surface area reduced GO (GO4) 3 to 5 μm size, 15 wt% oxygen, and 1 to 2 stacking layers.
- 5. Abalonyx's GO powder (GO5) 5 μm size and 32 wt% oxygen.
- 6. Graphene Supermarket's AO-2 graphene (graphene) 5 μm size and 5 nm stacking

2.2 Carbonization and Graphitization

A sealed tubing reactor setup was utilized to perform the carbonization of waste plastics and their GO-blends. The sealed tubing reactors were purged of air using compressed nitrogen through a quick-connect manifold, and then the reactor was placed inside a Thermolyne 21100 tube furnace. About 5 grams of pure plastics and Plastics + 2.5% GO were dry mixed and placed in the tubing reactor. The carbonization process was conducted under autogenic pressure at 600 °C for 3 hours in inert conditions. As PET is a charring plastic because of its oxygen content, it was carbonized at both autogenic pressure conditions in the tubing reactor as well as at atmospheric pressure. Subsequently, the obtained cokes were graphitized (GR) at a temperature of 2500 °C for 1 hour in a Centorr series 45 graphitization furnace. To maintain an inert graphitization environment, the graphitization furnace underwent three sequenced pump-down cycles, each reducing the pressure to less than 100 millitorr, followed by an Argon backfill. Carbon yields were measured for each sample as a percentage of precursor weight after the carbonization and graphitization steps.

2.3 Materials characterization

2.3.1 X-ray diffraction

The bulk-scale crystallinity of the graphitized samples has been analyzed using X-ray diffraction (XRD). A Malvern PANalytical Empyrean diffractometer featuring a Cu source (λ = 1.54 Å), parafocusing optics, and a PIXcel 3D detector was used for all measurements. The XRD measurements were conducted over the 2 θ range of 5 $^{\circ}$ – 90 $^{\circ}$, and subsequent peak deconvolutions were carried out using MDI JADE. To determine the in-plane crystallite diameter (La) and stacking height of graphene layers (Lc), the Scherrer equation with Ka and Kc values of 1.84 and 0.89, respectively, was applied to the deconvolutions exhibiting the lowest residuals.

2.3.2 Transmission electron microscopy

Transmission electron microscopy (TEM) imaged variations in morphology and nanostructure promoted by GO templating. Selected area electron diffraction (SAED) patterns were collected to assess the local crystallinity of the samples. An FEI Talos scanning/transmission electron microscope equipped with a FEG source with a resolution of 0.12 nm acquired images at 200 kV and 10 kX to 630 kX magnifications. To prepare the TEM samples, a small amount of ground sample powder was dispersed in ethanol through sonication and drop-casted onto a 300 mesh C/Cu lacey TEM grid.

2.3.3 Raman Spectroscopy

Raman spectroscopy provided a complementary technique to gain insights into the relative graphitic quality of heat-treated plastics versus GO-plastic composites. A Horiba LabRAM HR Evolution equipped with 600 groove/mm grating and a 488 nm laser generated the Raman spectra. To enhance the statistical significance of our findings, spectra were acquired using the DuoScanTM mode, allowing for rastering over a wider area or macro-spots. To mitigate potential oxidation or changes in nanostructure due to localized heating, a laser power of around 1 mW was consistently maintained throughout the measurements. To ensure the reliability of the analysis, more than three measurements were collected for each sample from various locations. Averaged results obtained from these multiple measurements are presented here.

2.3.4 Thermogravimetric Analysis – Differential Scanning Calorimetry

A comparative analysis of the differences between the carbonization of pure plastics versus GO-plastic blends was performed using Thermogravimetric Analysis/Differential Scanning Calorimetry (TGA-DSC). The TGA-DSC measurements were carried out using a NETZSCH STA-449 Jupiter TGA-DSC instrument. The samples were heated from room temperature to 600 °C at a heating rate of 25 °C/min, in an inert N₂ flow of 100 mL/min. TGA analysis was also used for estimating the purity (carbon%) of synthetic graphite samples by heating the samples in air from room temperature to 1000 °C in the air at 5 °C/min and measuring the residual non-carbon impurity percentage.

2.3.5 X-ray photoelectron spectroscopy

X-ray photoelectron spectroscopy (XPS) experiments analyzed the purity (carbon (%)) of the graphitized samples. Data collection was carried out using a Physical Electronics VersaProbe III apparatus featuring a monochromatic Al Kα X-ray source (energy: 1,486.6 eV) coupled with a concentric hemispherical analyzer. Measurements were conducted at a takeoff angle of 45° relative to the sample surface plane. To quantify the data, instrumental relative sensitivity factors were employed, which take into consideration both the X-ray cross-sectional area and the inelastic mean free path of the electrons. Three measurements from various locations were collected for each sample and the average values are reported.

2.4 Molecular Dynamics simulations

To identify possible differences in the carbonization process of the PE in the presence of graphene or graphene oxide, the following model systems were built – 1) Pure PE: with 50 PE polymer chains, 2) PE + GR: with 50 PE polymer chains and 5 layers of graphene, and 3) PE + GO: with 50 PE polymer chains and 5 layers of graphene oxide. The model molecules chosen to represent polyethylene, graphene, and graphene oxide are given in Figure 5 (a-d). In the case of all considered models, the periodic boundary conditions were applied and each graphene edge was connected through the periodic boundaries, effectively creating an infinite graphene structure. The ReaxFF C/O/N/H parameter set from Kowalik et al. ²⁸ was used to model the atomistic-scale interactions., using the AMS simulations software ³¹ to perform the Molecular Dynamics simulations. All simulation snapshots were generated with the use of the VMD software ³². In the

case of the constant pressure simulations (NPT), performed to equilibrate all systems at normal conditions (pressure 1 atm and temperature 300 K), a 100 fs damping parameter was used to control both, pressure and temperature, and 0.25 fs time step. For all elevated temperature simulations, the same damping parameter was applied, and a 0.1 fs time step was used together with a constant volume ensemble (NVT). All systems were heated from 300 K to 2800 K with a heating rate of 10 K/ps and kept at this elevated temperature of 2800K for 0.5 ns. This high temperature of 2800K was applied to accelerate the kinetics and observe the differences in carbonization of pure plastic versus plastic + additive systems within the ns time scale. Previously, MD simulations employing these parameters have demonstrated good agreement with experimental results in comparable systems $^{27,33-36}$.

Results

3.1 Carbon yield improvement

The incorporation of GO remarkably improved solid carbon yield for all waste plastics investigated in the study. Another advantage of including GO was that it dramatically reduced the autogenic pressure in the closed reactor. Carbonization of the pure waste plastic generated a maximum autogenic pressure of $\sim 800-1200$ psi; including GO reduced the maximum autogenic pressure generated in the reactor to less than ~ 400 psi. This reduced pressure indicates less volatile production and higher solid product yield due to the addition of GO.

3.1.1 Pure plastics versus their GO blends

The stabilization provided by GO markedly increased the carbon yield for all plastics. Figure 1 (a) shows a comparison of carbon yields of pure plastics after adding GO. The carbon yield increased between 35% to 235% with the highest increase observed for shredded PE film. Among pure plastics, HDPE shows the highest carbon yield attributable to its higher density and less branched crystalline structure, which generally allows the radicals generated during pyrolysis to be in closer proximity. Consequently, a higher radical proportion can combine and undergo subsequent cyclization and aromatization. As PET is an oxygen-containing resin, it gives measurable solid carbon yield even at atmospheric pressure of ~11% (not shown in Figure 1 (a)). Carbonization of

PET in a tubing reactor at autogenic pressure gives a carbon yield of ~20% which increases to ~33% after incorporating GO.

3.1.2 Effect of GO parameters on yield improvement

Figure 1 (b) shows carbon yields of PE versus PE blends with different GO additives. The addition of GO3 improved the carbon yield of pure PE by 38%. The addition of GO1 increased the carbon yield of pure PE by 233% i.e., doubling the O% of GO increased yield by six-fold. GO2 showed a yield increase close to that of GO1, indicating that the stacking height of GO additive does not influence yield enhancement significantly. This could be attributed to the gasification of oxygen function groups on GO during carbonization, which induces exfoliation and separation of all graphenic layers, making the initial stacking height inconsequential. If the GO layers were to remain stacked, it would alter the exposed sp2 surface area, subsequently affecting the yield. Comparing the addition of GO4 with GO3 shows that increasing the lateral size of GO ten times led to a ten-fold yield improvement. This observation supports sp2 templating by GO. Meanwhile, GO5 which has the highest O\% and largest lateral size showed the largest yield increase of ~480 % (not shown in Figure 1), further confirming the mechanisms of stabilization by GO. Directly addressing sp2 stabilization, the graphene having no oxygen functional groups but a 10X lateral size (not shown in Figure 1) improved the carbon yield of PE by 105%, further validating the important influence of lateral size variation in additives on their interactions with plastic materials. Quadrupling the GO1 loading from 2.5% to 10% increased the carbon yield further only marginally by $\sim 15\%$.

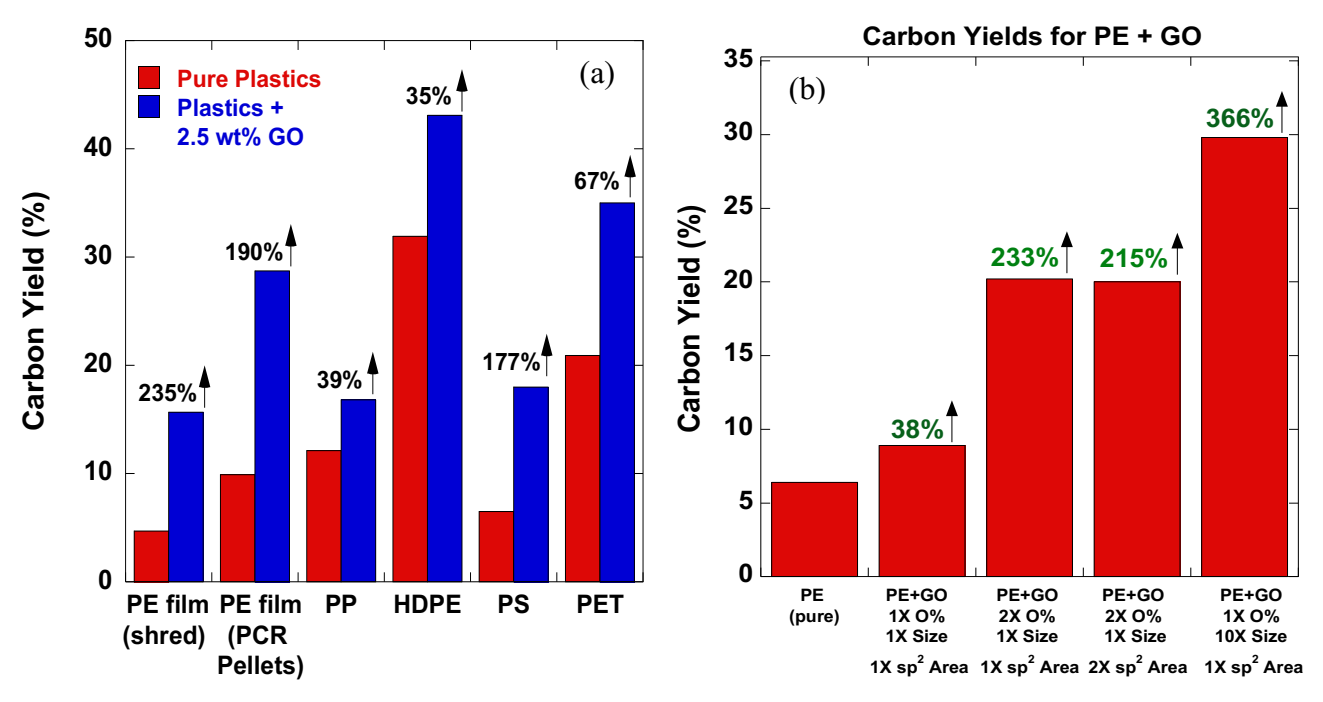


Figure 1. Carbon yields of (a) plastics versus GO-plastic blends, and (b) PE versus PE blends with different GO additives.

2.5 Graphitic quality assessment

3.2.1 Crystallite size assessment

In addition to the dramatic carbon yield increase, HDPE and PET showed crystallite size improvement with the addition of GO, whereas a trade-off was observed between carbon yield and crystallite size for the other plastics. This could be potentially due to crosslinking effects between plastic radicals and reactive radical sites produced by leaving oxygen groups on GO. Figure 2 shows comparative XRD-derived crystallite parameters of GR- pure plastic versus their GO blends. After the addition of GO, about $\sim 10\%$ improvement in L_a and L_c was observed for HDPE and PET while for other plastics, crystallite size parameters were smaller by 7 to 37%. To note, although the addition of GO slightly reduced the crystallite sizes for some plastics, all reported crystallite size values are significantly large and comparable to those observed for anthracene coke, which is known as a model graphitizable material with $Lc \sim 20$ nm and $La \sim 65$ nm. The comparative XRD spectra and the derived crystallite parameters are shown in supplementary

information. All samples showed 002 d-spacing values around ~3.38 Å, further confirming their graphitic nature. While the GO parameters had a substantial impact on the carbon yield of the plastic blends, the crystallite parameters consistently exhibited remarkably large across all GO additives, as detailed in the supplementary information.

It was found that even in the case of mixed plastic, graphitic carbon with high uniformity was obtained, as indicated by a single 002 peak in XRD. No discernible separation or contribution from multiple phases was observed. Moreover, the graphitic quality of the plastic blend (50% PE + 50% PS, not shown in Figure 2) was found to be better than individual PE and PS. The L_c , L_a , and 002 d-spacing for the blend were found to be 20 nm, 67.3 nm, and 3.36 Å respectively. The addition of GO to the plastic blend led to a ~190% increase in carbon yield, with crystallite parameters similar to that of the pure blend.

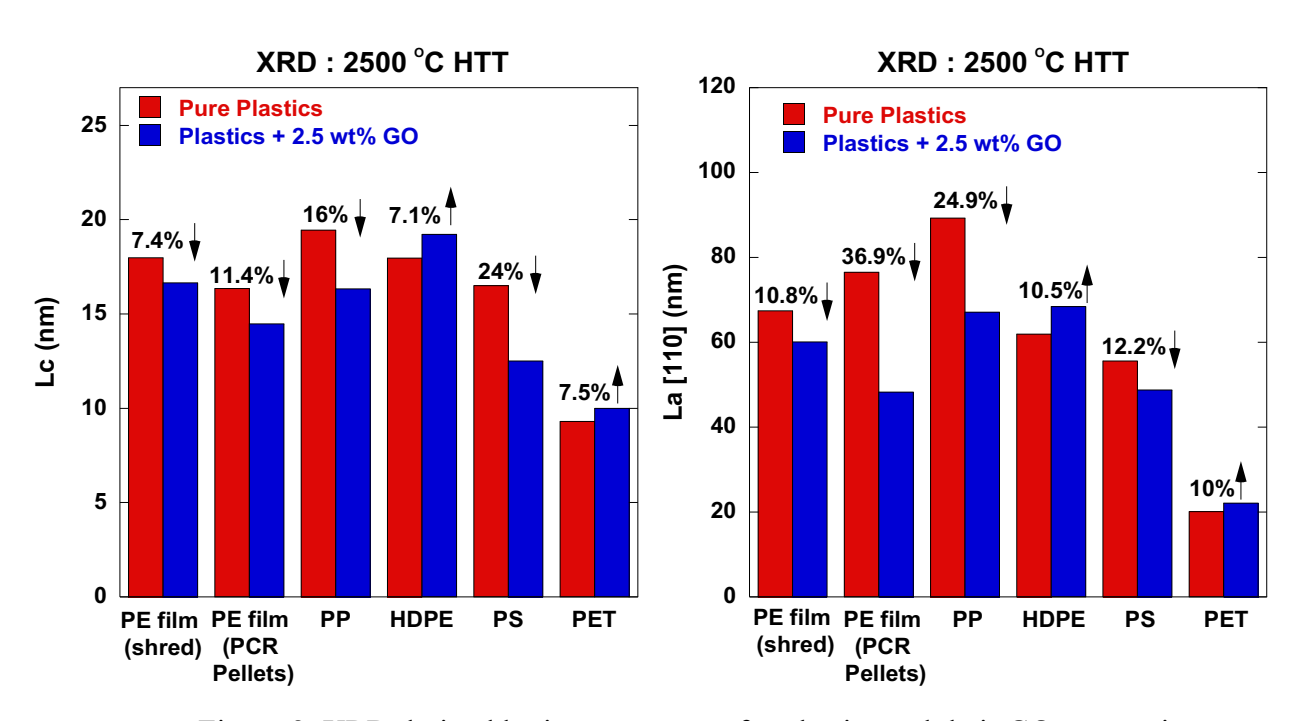


Figure 2. XRD derived lattice parameters for plastics and their GO composite.

3.2.1 Nanostructure assessment

TEM revealed remarkable differences between GR-pure plastics versus their GO composites. Templating by GO transformed the morphology in GR-HDPE from spherical aggregates of shells to thin flakes in GR-GO-HDPE as shown in Figure 3 (a and d). Furthermore, the nanostructure differences were also striking. Pure GR-HDPE showed nanostructure with a significant amount of crosslinking, curvature, and smaller domains, scrambled within spherical morphology that restricts lamellae extension as seen in Figures 3 (b-c). On the other hand, GR-GO-HDPE formed long continuous lamellae with large stacking height as seen in Figure 3 (e-f). SAED patterns given as insets in Figures 3 (e-f) further confirm the graphitic quality improvement with GR-HDPE having diffused and fuzzy ring patterns while GR-GO-HDPE shows a sharp ring pattern indicating higher crystallinity. The reason behind HDPE's sharp change in morphology and increase in graphitic quality could be its linear, less-branched chains aligning with the GO basal plane. Less branching may allow HDPE layers to align and decompose closer to GO's π -network. Such dependence on lower branching leading to higher hydrogen transfer ability has been seen in co-carbonization studies of coal and plastics ³⁷. This enhanced influence can extend to other layers better in HDPE than in other plastics again due to their compact assemblies. These changes in graphitic quality were confirmed by Raman analysis which is provided as supplementary information. The morphology and nanostructure of the other graphitized plastics and their composites exhibited similarity, as shown in the supplementary information.

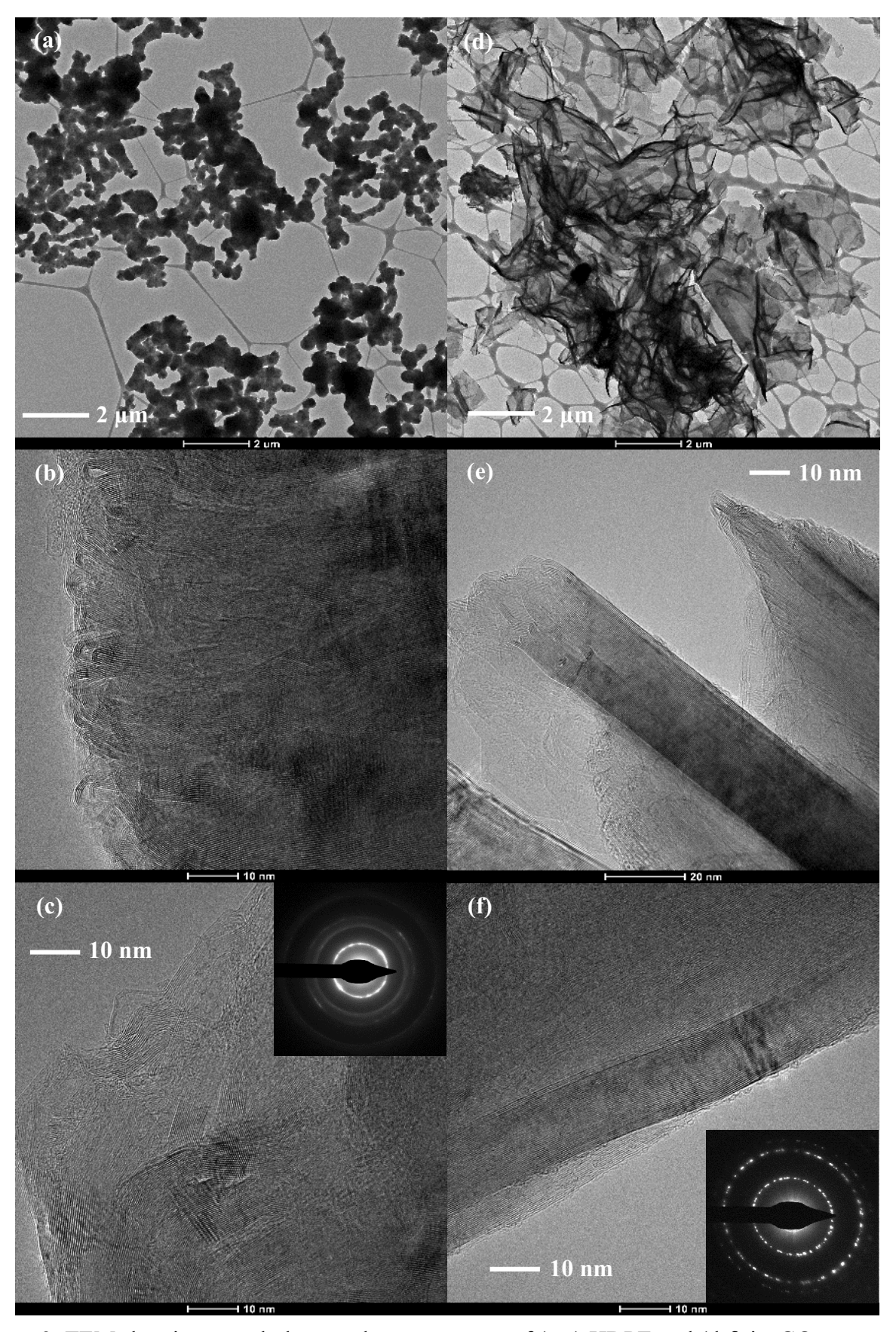


Figure 3. TEM showing morphology and nanostructure of (a-c) HDPE and (d-f) its GO composite.

3.3 Molecular Dynamics

The atomistic models and the snapshots at the equilibrium stage of the simulation can be found in the supplementary information. Figure 4 (a-c) provides the snapshots of PE + GO at different stages of carbonization. The initial phase of the carbonization was characterized by the bonding between polymer and GO shown in Figure 4 (a), while the carbonization led to the formation of all-carbon rings from the PE chains due to aromatization, which are shown as gray polygons in Figure 4 (b-c). Interestingly, these evolved aromatic clusters further bonded with the active sites on the GO during the carbonization. These noteworthy bonds, connecting graphene with a polymer matrix (highlighted in the yellow box) are shown in Figure 4 (c). The attachment of the evolved aromatic polymer matrix cluster to the GO is possible due to the presence of the reactive sites on the GO formed by the gasification of the oxygen functional groups during carbonization. This is validated by the changing proportion of the GO atomic composition as shown in Figure 4 (d). As one can see, the number of O atoms decreases with time, due to the gasification of functional groups, while the number of H and C atoms increases, due to the attachment of PE-derived aromatic clusters to GO.

To assess a change in the structure of the polymer matrix after carbonization, the RDFs for the polymer matrix C-C bonds are also compared, Figure 4 (e). The RDFs characteristic for the GR and GO-added system exhibit significantly higher peaks after carbonization compared to the PE. Furthermore, a noticeable shift of the RDF peak around ~ 2.5 Å to the left, indicates the formation of a higher number of aromatic rings in the case of the system with GR and GO addition compared to the pure PE. The snapshots of final structures for all models are given as the insets in Figure 4 (e) and Figure 4 (f) shows the formation of carbon rings at the end of carbonization in gray. All carbon atoms are represented as translucent spheres and sticks, cyan for carbon atoms, and red for oxygen, whereas all-carbon rings are represented as gray polygons. The quantitative assessment of the evolution of these carbon rings during the carbonization process is given in Figure 4 (g-i). These statistics show significantly higher ring formation in the presence of the additives, with the highest ring formation in the case of the GO system. This significantly higher ring formation results from PE reacting with the radical sites on the GO and helping in the "healing" process of the defected GO sheets. This "healing" was achieved through the formation of rings at the locations

previously occupied by oxygen functional groups, effectively filling in the "holes" left behind by their departure. Figure 4 (j-l) shows the top view of one of the GO layers with a red hexagon indicating the newly formed rings through the healing process. The active sites present on GO play a crucial role in activating the polymer matrix, leading to a substantial increase in their interaction. The differences in the composition of gas produced during the carbonization of pure polymer versus additive systems are provided in the supplementary information.

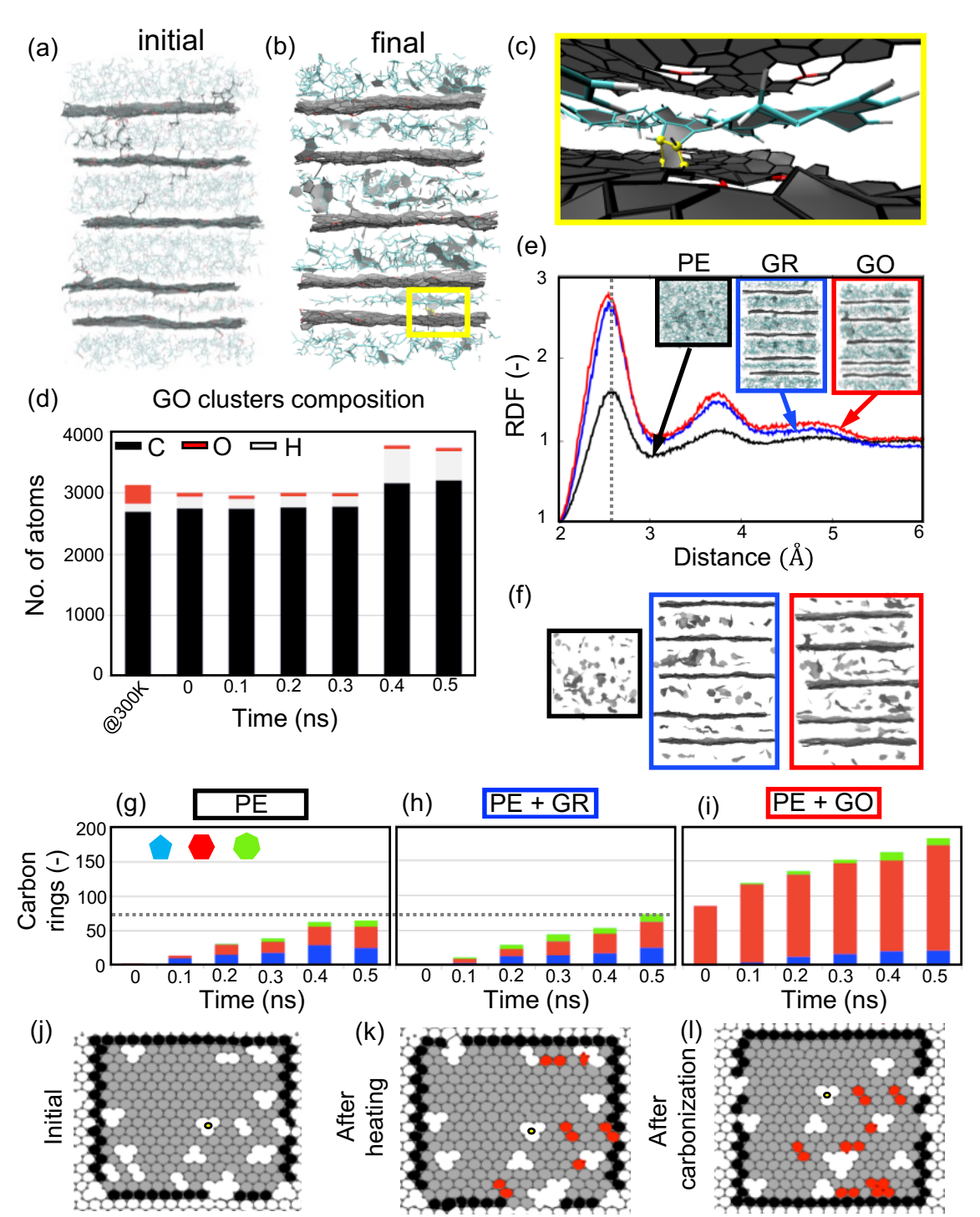


Figure 4. Atomistic models for the structure observed for the PE + GO system (a) at the beginning of the carbonization, (b) at the end of the carbonization simulations, (c) the zoomed-in region to this junction between the GO and the evolved carbon cluster, (d) stacked bar plot showing the time evolution of the atoms statistics for GO; (e) RDF for the all polymer carbon atom pairs for pure polymer versus additive systems, (f) final snapshots of carbonization with carbon rings shown in gray; the bar plots of the number of all-carbon rings evolved during the carbonization (g-i) PE versus additive systems; (j-l) top view GO highlighting the healing process at different stages of carbonization. All initial rings are highlighted in gray and the rings at the box boundary appear in black. The C-C bonds in the polymer matrix and evolved aromatic clusters are highlighted in cyan, and any C-C bonds for the GR/GO, including the bond between PE radicals and the active sites on the GO are represented by black sticks.

3.4 Improvements in carbonization reactions and proposed mechanisms of interaction

Figure 5 provides the TGA-DSC analysis of pure versus GO-blended PE and HDPE, respectively. The addition of GO led to a notable carbonization yield increase in excess of GO's contribution at the end of the temperature ramp, from ~0% in pure PE to ~10% in PE + 2.5% GO as seen in Figure 5 (a). Figure 5 (b) shows the stabilizing nature of GO wherein the DSC profile of the GO-PE blend compared to pure PE starts at a higher DSC heat flow value but goes significantly lower at the end of the carbonization temperature. This indicates that GO promotes endothermic reactions such as melting, chain unzipping, etc. in the initial lower temperature range and later leads to a higher extent of exothermic reactions associated with stable products. Indeed, the DDSC profile of GO-PE blend shows two noteworthy peaks associated with exothermic reactions around 400 °C and 500 °C which are absent in pure PE. The correlation between differences in carbonization reactions as observed in TGA-DSC and their impact on graphitizability has previously been validated ³⁸. To note, these improvements were observed in TGA-DSC that operates at atmospheric pressure. They can be expected to occur to a substantially higher extent under autogenic pressure in the tubing bomb apparatus where the contained gases continue to react under GO's influence.

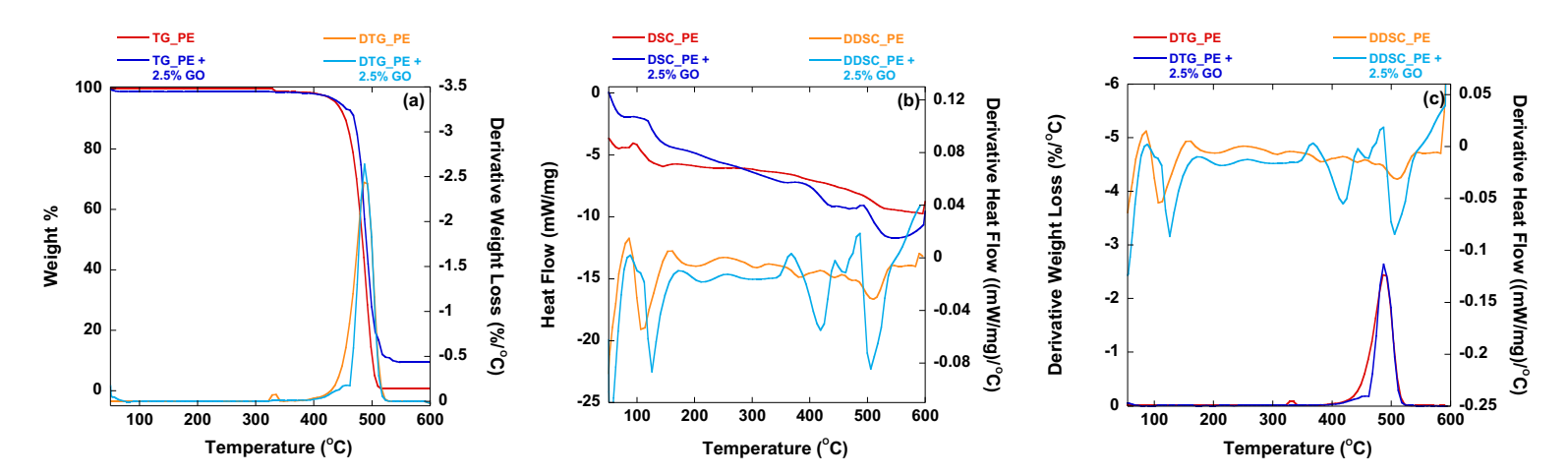


Figure 5. An overlay of (a) TG and DTG, (b) DSC and DDSC, and (c) DTG and DDSC for carbonization of pure PE versus PE + 2.5% GO.

Based on the additive parameter dependence of yield, molecular dynamics, and TGA-DSC, Figure 6 provides visual illustrations of the three proposed interaction mechanisms which are detailed in the discussion section. The snapshots from MD simulations supporting the mechanisms are provided in the right-hand column of Figure 6.

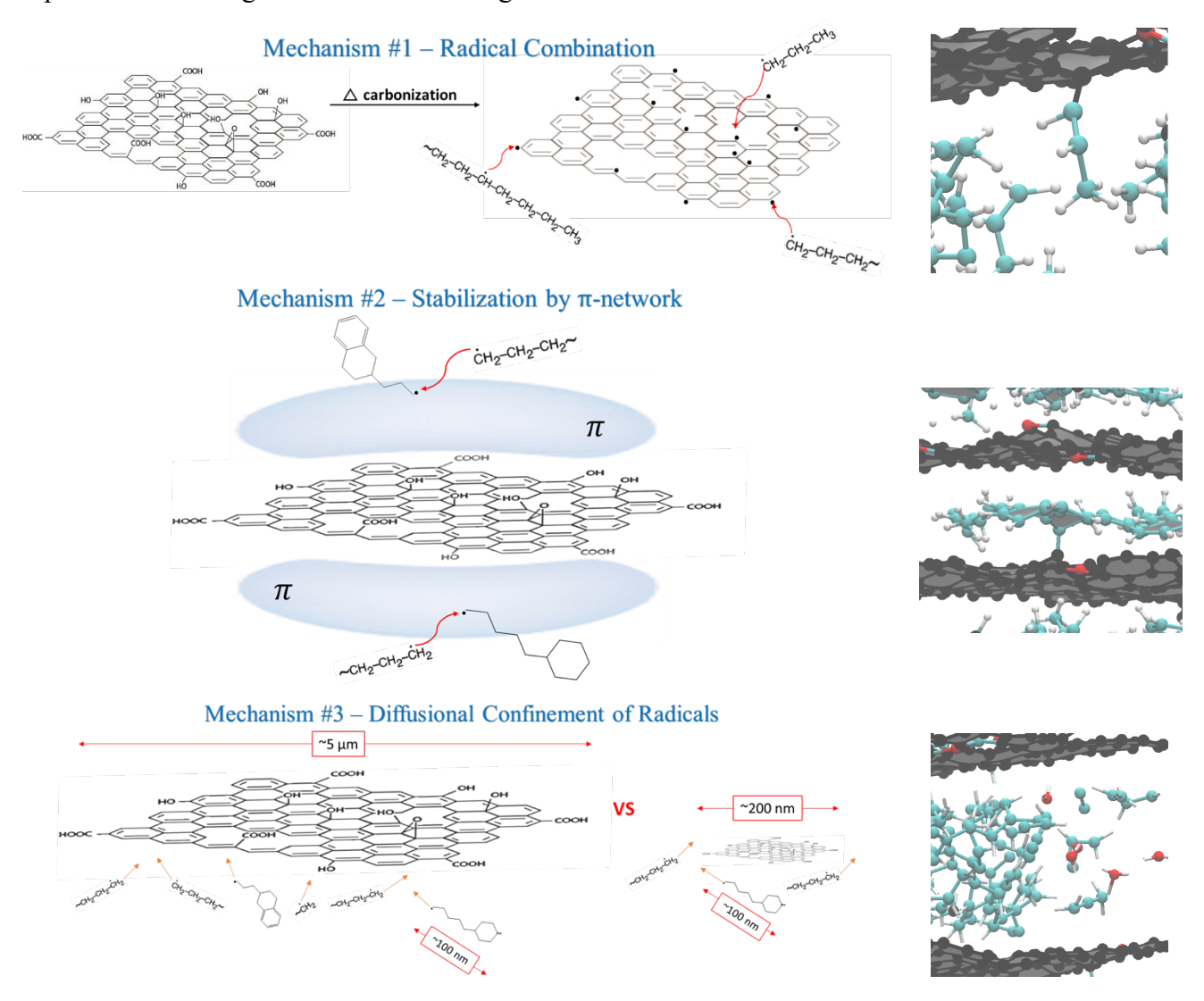


Figure 6. Visual illustrations of the interaction mechanisms between plastic and GO during carbonization.

4. Discussion

Pure plastics have extremely low carbon yields as they go through chain unzipping and β-bond scission when heated to produce light gases. The stabilization provided by GO additive in a sealed reactor remarkably improves the solid carbon yield for all plastics and as much as ~250% for PE. Analysis of the yield improvement with different GO additives provided insights into the mechanisms of interaction between plastic and GO during pyrolysis. GO improves the carbon yield of plastics by three main mechanisms: 1) radical combination reactions between polymer and GO radicals, 2) stabilization of polymer radicals by GO's π -network, and 3) diffusional confinement of polymer radicals. The visual illustrations of these mechanisms are provided in Figure 6. These mechanisms can be influenced by the composition, (i.e., oxygen (%)), stacking height, and lateral size of GO, respectively. During carbonization, oxygen functional groups on GO gasify, leaving behind radicals on GO that undergo radical combination reactions with the surrounding polymer radicals. The MD simulations confirmed that the pyrolyzing polymer radical chains bond with the active sites on the GO and induce "healing" of the GO through ring formation. If the polymer radicals generated during carbonization are not stabilized, they continue to crack into smaller fragments to yield light gases and little solid carbon. The stabilization provided by GO's π -network can increase the lifetime of the polymer radicals, so that they can undergo aromatization and growth, rather than cracking. Notably, GO can also aid the alignment of these aromatics and subsequent ordered growth via π - π interactions. This interpretation of better structure and ordering through π - π interactions is supported by an improved RDF observed in MD simulations of the additive systems. During carbonization, smaller gaseous polymer radicals are generated, while large solid GO sheets stabilize them and confine their movement. This promotes inter-radical reactions, leading to cyclization, aromatization, and subsequent concatenation reactions. The carbon yield improvement was also observed with graphene additive having no oxygen but a large lateral size, further supporting the importance of diffusional confinement and stabilization mechanisms. Indeed, the TGA-DSC analysis and MD simulations confirm that the embedded GO promotes endothermic reactions such as melting, chain unzipping, etc. in the initial lower temperature range and later leads to a higher extent of exothermic reactions associated with stable products. Aligned with TGA-DSC results, MD simulations showed that the polymer unzipping is accelerated through interaction with additives.

In addition to the remarkable yield increase, the crystallite size and nanostructure improve markedly for HDPE and PET. A trade-off between carbon yield and crystallite size was noted for other plastics, likely due to the mild crosslinking responsible for the observed yield increase. The cokes produced from all recycled plastics are highly graphitizable, with crystallite parameters comparable to the industrial graphitization standard – anthracene coke. The synthetic graphites exhibit thin flakes characterized by long continuous lamellae and a large stacking height. The particular blend of waste plastics (50% PE + 50% PS) forms a graphitic carbon with a uniform crystalline phase and slightly better crystallite sizes than the separated plastics. This phenomenon can be attributed to the synergistic interactions between the aliphatic structure of PE and the aromatic framework of PS, a well-established concept in the industrial production of graphites from pitches.

After graphitization, all the heteroatoms leave and remarkably high purity (~100% carbon) synthetic graphite was obtained. This was validated by X-ray photoelectron spectroscopy and TGA oxidation analysis, as detailed in the supplementary information. This study demonstrates the versatility of recycled plastics in various forms, including flake, reprocessed pellets, foams, colored variants, and even mixed compositions, as viable feedstocks for obtaining uniform crystalline-phase graphitic carbon. Such versatility holds significant importance, as it addresses major challenges in plastic recycling, specifically the issues of separation and transportation. More broadly this work outlines a solution intersecting three challenges – 1) declining availability of graphitic carbon precursors, 2) projected supply shortfall driven by rapidly rising graphite demand for batteries, and 3) growing abundance of plastic waste. The approach reduces plastic waste and the CO₂ footprint associated with the manufacture of graphitic carbons by displacing mining for natural graphite or oil recovery and refining for aromatic feedstocks. Beyond their application in batteries, these waste plastic-derived carbons can be used as polymer additives for improving mechanical properties, conductivity, abrasion resistance, increased protection from UV, pigmentation, etc. Transforming excess plastic waste into graphitic carbons can play a pivotal role

in advancing the shift towards renewable energy sources, simultaneously mitigating pollution, lowering costs, and curbing CO₂ emissions.

Conclusion

In this initial study, six commercially recycled plastics and blends with GO were evaluated for their comparative carbon yield and graphitic quality. GO provided excellent stabilization through the radical sites formed by the leaving groups. The key advantage of GO as an additive is that it netted a substantial increase in carbon yields, nearly 250% in some plastics. In addition to the significant increase in carbon yield, the addition of GO enhanced crystallite size and graphitic quality for HDPE and PS. Across all recycled plastics, the carbons exhibited remarkable graphitizability, featuring crystallite parameters on par with those observed in the model graphitizable material, namely anthracene coke. The synthetic graphite derived from waste plastic exhibited thin flakes with well-stacked, long, and continuous lamellae. These features are advantageous to anode material in LIBs. The interaction mechanisms between graphenic additives and waste plastics leading to improved yield and quality of graphitic carbon were discovered through collaborative experimental investigations and atomistic-scale molecular dynamic simulations. [say something here about the interaction mechanisms in Figure 6 and how joint experiment/theory helped us to formulate these mechanisms] This demonstrated production of high-value carbons from consumer single-use waste plastics will boost recycling and enable other related uses for carbon materials formed from plastic waste.

Acknowledgments

This material is based upon work supported by the National Science Foundation under Grant CBET-2309333.

References

- U.S. generates more plastic trash than any other nation, report finds.
 https://www.nationalgeographic.com/environment/article/us-plastic-pollution. Accessed
 November 25, 2021.
- 2. Accelerating plastic recovery in the United States | McKinsey.

- https://www.mckinsey.com/industries/chemicals/our-insights/accelerating-plastic-recovery-in-the-united-states. Accessed November 27, 2021.
- 3. Lindwall C. Single-Use Plastics 101. https://www.nrdc.org/stories/single-use-plastics-101#what. Published 2020. Accessed February 9, 2023.
- 4. Containers and Packaging: Product-Specific Data | US EPA. https://www.epa.gov/facts-and-figures-about-materials-waste-and-recycling/containers-and-packaging-product-specific-data#C&POverview.
- 5. Plastic pollution facts and information. 2019. https://www.nationalgeographic.com/environment/article/plastic-pollution#:~:text=Every year%2C about 8 million,of coastline around the world.
- 6. Eriksen M, Cowger W, Erdle LM, et al. A growing plastic smog, now estimated to be over 170 trillion plastic particles afloat in the world's oceans—Urgent solutions required. *PLoS One*. 2023;18(3):e0281596.
- 7. Northern Graphite | The Future of North American Graphite Production.
 http://www.northerngraphite.com/about-graphite/the-graphite-supply-problem/. Accessed
 November 27, 2021.
- 8. Yang L, Yang L, Xu G, et al. Separation and recovery of carbon powder in anodes from spent lithium-ion batteries to synthesize graphene. *Sci Rep.* 2019;9(1):1-7.
- 9. Kamali AR, Fray DJ. Review on carbon and silicon based materials as anode materials for lithium ion batteries. *J New Mater Electrochem Syst.* 2010;13(2):147-160.
- 10. Yan J, Li W, Wang R, et al. An in Situ Prepared Covalent Sulfur–Carbon Composite Electrode for High-Performance Room-Temperature Sodium–Sulfur Batteries. *ACS Energy Lett.* 2020;5(4):1307-1315.
- 11. Lempriere M. Could graphene batteries change the face of graphite mining? https://www.mining-technology.com/features/graphene-batteries-change-face-graphite-mining/. Published 2018. Accessed January 9, 2023.

- 12. Berktas I, Hezarkhani M, Poudeh LH, Okan BS. Recent developments in the synthesis of graphene and graphene-like structures from waste sources by recycling and upcycling technologies: a review. *Graphene Technol.* 2020:1-15.
- 13. Chemical Recycling 101. https://www.bpf.co.uk/plastipedia/chemical-recycling-101.aspx# Toc31632536.
- 14. Bockhorn H, Hornung A, Hornung U. Mechanisms and kinetics of thermal decomposition of plastics from isothermal and dynamic measurements. *J Anal Appl Pyrolysis*. 1999;50(2):77-101. doi:10.1016/S0165-2370(99)00026-1
- 15. Kodera Y, McCoy BJ. Distribution kinetics of plastics decomposition. *J Japan Pet Inst*. 2003;46(3):155-165. doi:10.1627/jpi.46.155
- 16. Zeng WR, Chow WK, Yao B. Chemical kinetics and mechanism of polystyrene thermal decomposition. *Fire Saf Sci.* 2007;7:128.
- 17. Tsuchiya Y, Sumi K. Thermal decomposition products of polypropylene. *J Polym Sci Part A-1 Polym Chem.* 1969;7(7):1599-1607.
- 18. Choi D, Jang D, Joh H-I, Reichmanis E, Lee S. High performance graphitic carbon from waste polyethylene: thermal oxidation as a stabilization pathway revisited. *Chem Mater*. 2017;29(21):9518-9527.
- 19. Panahi A, Sun X, Song G, Levendis YA. On the Influences of Carrier Gas Type and Flow Rate on CVD Synthesis of CNTs from Postconsumer Polyethylene. *Ind Eng Chem Res*. 2020;59(31):14004-14014.
- 20. Wen Y, Kierzek K, Chen X, et al. Mass production of hierarchically porous carbon nanosheets by carbonizing "real-world" mixed waste plastics toward excellent-performance supercapacitors. *Waste Manag.* 2019;87:691-700.
- 21. Ko S, Kwon YJ, Lee JU, Jeon Y-P. Preparation of synthetic graphite from waste PET plastic. *J Ind Eng Chem.* 2020;83:449-458.

- 22. Lee G, Park SI, Shin HY, Joh H-I, Kim S-S, Lee S. Simultaneous reactions of sulfonation and condensation for high-yield conversion of polystyrene into carbonaceous material. *J Ind Eng Chem.* 2023;122:426-436.
- 23. BU-309: How does Graphite Work in Li-ion? Battery University. https://batteryuniversity.com/article/bu-309-how-does-graphite-work-in-li-ion.
- 24. Saha B, Schatz GC. Carbonization in polyacrylonitrile (PAN) based carbon fibers studied by ReaxFF molecular dynamics simulations. *J Phys Chem B*. 2012;116(15):4684-4692.
- 25. Saha B, Furmanchuk A, Dzenis Y, Schatz GC. Multi-step mechanism of carbonization in templated polyacrylonitrile derived fibers: ReaxFF model uncovers origins of graphite alignment. *Carbon* 2015;94:694-704. doi:10.1016/j.carbon.2015.07.048
- 26. Desai S, Li C, Shen T, Strachan A. Molecular modeling of the microstructure evolution during carbon fiber processing. *J Chem Phys.* 2017;147(22).
- 27. Zhang L, Kowalik M, Gao Z, et al. Converting PBO fibers into carbon fibers by ultrafast carbonization. *Carbon* 2020;159:432-442.
- 28. Kowalik M, Ashraf C, Damirchi B, Akbarian D, Rajabpour S, Van Duin ACT. Atomistic scale analysis of the carbonization process for C/H/O/N-based polymers with the ReaxFF reactive force field. *J Phys Chem B*. 2019;123(25):5357-5367.
- 29. Zhu J, Gao Z, Kowalik M, et al. Unveiling carbon ring structure formation mechanisms in polyacrylonitrile-derived carbon fibers. *ACS Appl Mater Interfaces*. 2019;11(45):42288-42297.
- 30. Kato T, Yamada Y, Nishikawa Y, Ishikawa H, Sato S. Carbonization mechanisms of polyimide: Methodology to analyze carbon materials with nitrogen, oxygen, pentagons, and heptagons. *Carbon* 2021;178:58-80.
- 31. Baerends EJ, Ziegler T, Autschbach J, et al. SCM, Theoretical Chemistry, Vrije Universiteit, Amsterdam, The Netherlands. 2017.

- 32. Humphrey W, Dalke A, Schulten K. VMD: visual molecular dynamics. *J Mol Graph*. 1996;14(1):33-38.
- 33. Li X, Zheng M, Ren C, Guo L. ReaxFF molecular dynamics simulations of thermal reactivity of various fuels in pyrolysis and combustion. *Energy & Fuels*. 2021;35(15):11707-11739.
- 34. Vashisth A, Kowalik M, Gerringer JC, Ashraf C, Van Duin ACT, Green MJ. ReaxFF simulations of laser-induced graphene (LIG) formation for multifunctional polymer nanocomposites. *ACS Appl Nano Mater*. 2020;3(2):1881-1890.
- 35. Gao Z, Zhu J, Rajabpour S, et al. Graphene reinforced carbon fibers. *Sci Adv*. 2020;6(17):1-11. doi:10.1126/sciadv.aaz4191
- 36. Gallegos I, Kemppainen J, Gissinger JR, et al. Establishing Physical and Chemical Mechanisms of Polymerization and Pyrolysis of Phenolic Resins for Carbon-Carbon Composites. *Carbon Trends*. 2023:100290.
- 37. Díez MA, Barriocanal C, Álvarez R. Plastic wastes as modifiers of the thermoplasticity of coal. *Energy and Fuels*. 2005;19(6):2304-2316. doi:10.1021/ef0501041
- 38. Gharpure A, Vander Wal RL, Pisupati S. Synthetic Pitch from Solvent Extraction of Coal as a Source for High-Quality Graphite. *C.* 2023;9(2):56.